

Analyses on flow and heat transfer performance and of heat exchanger with continuous helical baffles

Jiazhu Zou, Fengwei Yuan*, Qian Deng

College of Mechanical Engineering, University of South China, Hengyang 421001, Hunan, China

Received 1 October 2014, www.cmnt.lv

Abstract

A numerical simulation for heat exchanger with continuous helical baffles was carried out. The study focuses on the effects of helix angle on flow and heat transfer characteristics, and heat exchanger performance is evaluated by entropy generation number based on the analysis of the second law of thermodynamics. The results show that both the shell-side heat transfer coefficient and pressure drop decrease with the increase of the helix angle at certain mass flow rate. The latter decreases more quickly than the former. The tangential velocity distribution on shell-side cross section is more uniform with continuous helical baffles than with segmental baffles. The axial velocity at certain radial position decreases as the helix angle increases in the inner region near the central dummy tube, whereas it increases as the helix angle increases in the outer region near the shell. The heat exchange quantity distribution in tubes at different radial positions is more uniform at larger helix angle.

Keywords: continuous helical baffles, heat exchanger, helix angle, entropy generation, numerical simulation

1 Introduction

The conventional shell and tube heat exchanger most used in the arch baffles, and the shell side fluid flows along the side with large pressure. There are the flow and heat transfer dead regions in the shell side. It is not only easy scaling, but that the high velocity easily induced vibration of heat exchanger tube and shorten the service life. For this kind of situation, from the Angle of the change of baffle plate arrangement, put forward the thought of the spiral baffle plate heat exchanger, the application in the shell side of the heat exchanger along the axial of the spiral baffle plate structure, made fluid helical plunger flow. Flow uniform stability, thus overcome the bow baffle plate heat exchanger of the above shortcomings. Existing research shows that compared with the bow baffle plate heat exchanger, spiral baffle plate heat exchanger when the shell side of the same flow unit pressure drop of the heat transfer coefficient is higher, especially for the high degree of double fluid, its advantage is more outstanding.

Most of current research of the spiral baffle plate heat exchanger to apply a set of method and the heat exchange tube axial Angle of fan-shaped certain plane board to lap, approximate spiral surface formation, called the continuous helical baffle plate. Although it is easy to manufacture installation, but this kind of structure because of the discontinuity of the baffle plate and the triangular space is formed between two adjacent frames. The shell side fluid in the region will form a short circuit leakage flow, lead to flow deviation from the ideal spiral flow, thus affecting the performance of heat transfer in the heat exchanger.

To make the shell side fluid to achieve relatively smooth continuous spiral flow, baffle plate should be continuous

spiral curved surface, called continuous helical baffles. Baffle plate in the shell on the formation of the spiral curve tangent with the angle β between the cross section is defined as the continuous helical baffle helical angle.

$$\beta = \arctan\left(\frac{H_s}{\pi D_s}\right)_{\varphi} \quad (1)$$

The shell side of the helical angle determines the Angle between the direction of fluid flow and heat exchange tube bundle, boundary layer thickness and the flow characteristics and so on, in the shell inside diameter must, helical angle determines the cross-section of the shell side of the pitch and circulation, directly affect the shell side heat transfer and resistance properties. So, helical angle is reflecting the continuous helical baffle heat exchanger thermal performance of the important parameters.

Experimental study of continuous helical baffle heat exchanger is made the high installation costs, cycle is long, and not easy to get the distribution of the shell side quantities, this paper established the continuous helical baffle heat exchanger of three-dimensional physical model. A numerical simulation for heat exchanger with continuous helical baffles was carried out by using commercial codes of ANSYS CFD 12.0. The study focuses on the effects of helix angle on flow and heat transfer characteristics, and heat exchanger performance is evaluated by entropy generation number based on the analysis of the second law of thermodynamics.

2 The physical model and geometric dimensions

The continuous helical baffle heat exchanger shell side application, because in the actual processing baffle plate screw

*Corresponding author e-mail address: 1057487156@qq.com

surface tangent direction of the centre and the shell axial Angle is very small, drilling difficulties, usually equipped with centre false tube helical surface centre position, no false tube fluid flow, the numerical simulation model of heat exchanger is applied with centre of false tube structure. Continuous helical baffle heat exchanger the calculation area physical model as shown in Figure 1, the basic structure size reference GB 151-151, as shown in Table 1.

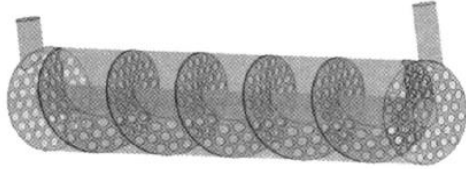


FIGURE 1 Physical model calculation area

TABLE 1 Geometric parameters of heat exchanger

Parameter	Value
inner diameter of shell/mm	207
diameter of central dummy tube/mm	60
diameter of tube/mm	19
central distance of tubes/mm	25
arrangement of tubes	regular triangle
number of tubes	48
helix angle/(°)	10,20,30,40,45
helical pitch/mm	115,237,376,546,650
tube length/mm	1750

3 Mathematical model and numerical simulation method

3.1 TURBULENCE MODEL AND THE CONTROL EQUATION

Continuous helical baffle heat exchanger shell side turbulent pulsating flow with spiral flow interaction, to show high levels of anisotropy and sensitivity to the streamline curvature, so numerical simulation using RNG k model, its strong streamline curvature, the vortex and has good performance of rotating calculation, at the same time in close to the constant application of standard wall function method.

General control equation for related physical quantities

$$\text{div}(\rho U \phi) = \text{div}(\Gamma_{\phi} \text{grad} \phi) + S_{\phi} \quad (2)$$

Substituting different general variables ϕ , Equation (2) to show the continuity equation, momentum equation and energy equation and the equation of $k - \varepsilon$, the generalized diffusion coefficient Γ_{ϕ} and generalized the values S_{ϕ} in the source term is corresponding to each equation.

3.2 WORKING MEDIUM FLOW AND BOUNDARY CONDITIONS

Shell side working medium for heat conduction oil, its steady turbulent flow in the shell side channel. Because of heat conduction oil, the degree of value changing with temperature is bigger, it is a function of temperature to the fitting $\mu = 5.18125 \times 10^{-6} T^2 - 3.69 \times 10^{-3} T + 0.66233$, the rest of the physical parameters of constant. In the working medium

is water passes and physical parameters are constant. Both gravity, thermal buoyancy lift and clear heat dissipation.

To determine the appropriate boundary conditions on the physical model of simplified. A given shell side inlet mass flow rate M_s , temperature $T_{s,i} = 353.15k$ and turbulence intensity $I = 5\%$; Tube side population rate constant, $v = 1.5m \cdot S^{-1}$ define temperature $T_{s,i} = 353.15k$ and turbulence intensity $I = 5\%$. The shell side and tube side exports are pressure outlet boundary, given the recycling of static pressure and the appropriate conditions. No sliding surface is defined as the heat exchange tube impermeable solid wall, the application of coupling boundary conditions of cold and hot fluid heat transfer FGC calculation; Baffle plate and shell wall impermeable solid wall is defined as adiabatic without sliding.

3.3 MESHING WITH NUMERICAL SIMULATION METHOD

The shell side of the continuous helical baffle heat exchanger internal structure is complex, so the application of tetrahedron and pyramidal unstructured meshing; in the application passes hexahedron mesh. Selected unit number is respectively 11.82 million, 14.92 million, 17.78 million, 3 sets of grid independence test, when $M_s = 10Kg \cdot S^{-1}$, the spiral Angle of 40° of continuous helical baffle heat exchanger by the 3 sets of the grid to calculate the shell side of heat transfer coefficient and pressure drop, respectively in the import and export $446.1W \cdot m^{-2} \cdot K^{-1}$, $70164.1Pa$, $452.2W \cdot m^{-2} \cdot K^{-1}$ and $65891Pa$, $456.5W \cdot m^{-2} \cdot K^{-1}$ and $65035.9Pa$, after the 2 sets of grid computing results are within 2%. Considering calculation accuracy and efficiency, choose 2 sets of grid computing.

Finite volume method was applied to calculate area and control equations are dispersed and solving, define the convergence condition of the equation of average residual error absolute value is less than 1.0×10^{-5} .

3.4 NUMERICAL SIMULATION VALIDATION

Applying the method of continuous helical baffle heat exchanger are simulated, and the results were compared with the experimental data. Figures 2 and 3 shows the shell side pressure drop simulation value and experiment value deviation for 13.800-21.2%, the shell side heat transfer coefficient of deviation for the simulation value and experiment value 7.8% - 8%, deviation in a reasonable scope, the validity of the numerical simulation method presented in this paper.

Besides inevitable error of measurement, numerical simulation of the heat exchanger of simplified model and boundary conditions may cause the deviation between the numerical simulation results with the experimental data, for example, numerical simulation of the model ignores the baffle plate and shell and the leakage flow between heat exchange tube, baffle plate and shell wall is simplified to adiabatic boundary condition, etc.

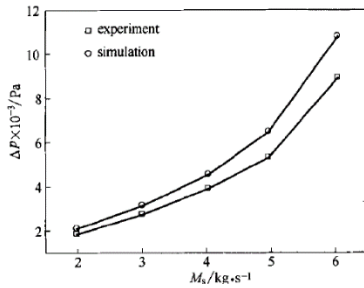


FIGURE 2 Shell side pressure drop experimental value compared with the simulation values

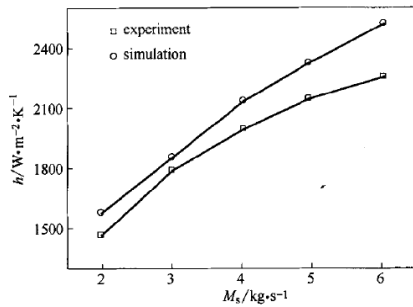


FIGURE 3 Shell side heat transfer coefficient of the experimental value and simulation value comparison

The effect of leakage flow and significantly with the increase of shell side flow, so the deviation between the simulated results with the experimental data with the flow rate increases.

4 The results of numerical simulation and analysis

4.1 SHELL SIDE SCREW CHANNEL AXIAL DISTRIBUTION OF CONVECTIVE HEAT TRANSFER

Continuous helical baffle heat exchanger shell side fluid in the shell, baffle plate, centre pipe and heat exchange tube wall of channel flow, heat transfer along the flow direction of the development process, with the development of the fluid mechanics was conducted at the same time. To high pr, such as heat conduction oil fluid, in fully developed section, heat transfer rate have also been fully developed. So, the shell side of the can from cross section along the axial distribution of local heat transfer coefficient on the shell side of the judgment convective heat transfer full development period of spiral channels.

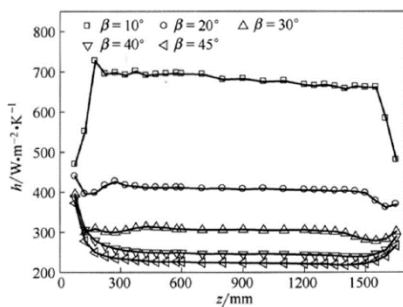


FIGURE 4 Screw channel and the distribution of local heat transfer coefficient along the axial direction

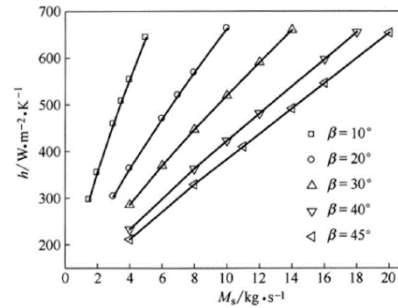


FIGURE 5 Shell side heat transfer coefficient changing with the flow

To decorate with continuous helical baffle and processes do not include the shell The shell side of the outlet pipe of the channel for the screw channel, can see from Figure 4, the shell side mass flow rate is equal to ($M_s = 4Kg \cdot S^{-1}$). The screw channel and local heat transfer coefficient h and decreased with the increase of helical Angle. This is because the spiral Angle increases means that the circulation of the shell side of the pitch increases, sectional area increase, results in the decrease of flow velocity, h is reduced.

Helix Angle is not at the same time, the axial distribution of h is very different: the spiral Angle of 10° , h decreased slightly after a sharp increase is seen at the inlet section of the first, and then its value changed little, marked the convective heat transfer into the full development stage, in the export section h drastically reduced; Spiral Angle of 20° and 30° , h in the inlet and outlet section shows the trend of increase with the decrease of, after first; Spiral Angle of 40° and 45° , h in inlet and outlet, respectively is the decrease and increase the monotonicity of the trend. This is because of the inlet and outlet of the spiral channel flow at the inlet and outlet of the cross-sectional area by the baffle plate and tube plate of the distance between the decision, and fully development period of the circulation of sectional area is determined by the baffle plate pitch, when the helix Angle is small, the former is greater than the latter, made of import and export as full development period of high flow velocity, and can lead to the development of import and export of h is less than fully; with the increase of helical Angle, the situation is the opposite.

In the comprehensive analysis, fluid flow people screw channel after about 1 times the length of the pitch of the part is import section, flow channel is about 0.75 times the length of the pitch before the part of the period for export, import and export for the part between the convective heat transfer full development period.

4.2 FULL DEVELOPMENT PERIOD OF HEAT CONVECTION OF SHELL SIDE HEAT TRANSFER AND RESISTANCE PERFORMANCE

As shown in Figures 5 and 6, the shell side of the same mass flow, the shell side heat transfer coefficient of convective heat transfer full development period of h and pressure drop per unit length Δp_m are reduced with the increase of helical Angle. When $M_s = 4Kg \cdot S^{-1}$ compared with the spiral

Angle of 10°, h and Δp_m decrease respectively 34.4% and 87.9% at 20° and respectively lower 48.3% and 96.5% at 30°, respectively reduce 57.9% and 98.6% at 40°, respectively 61.7% and 99.1% at 45°, the lower the trend will be increased with the increase of flow rate is more and more significant.

This is because, on the one hand, the shell side of the pitch and circulation area increases with the increase of helical Angle, reduce with traffic flow and h and Δp_m so reduce. The shell side of the small spiral Angle, on the other hand, closer to the fluid flow form horizontal tube bundle, same velocity when the heat transfer effect is better. But also inevitably bring large pressure loss. Because along with the increase of helical Angle, Δp_m lower margin than h , significantly, Figure 7 shows the shell side heat transfer and resistance performance will increase along with the increase of helical Angle.

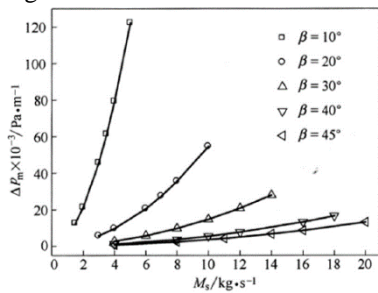


FIGURE 6 Shell side pressure drop per unit length along with the change of flow rate

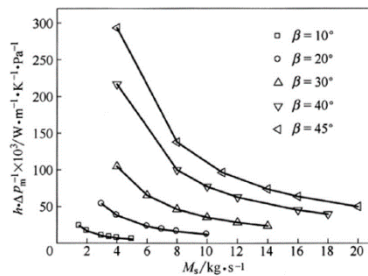


FIGURE 7 Shell side comprehensive performance along with the change of flow

4.3 THE SHELL SIDE VELOCITY DISTRIBUTION

Fluid in the shell side channel spiral flow, the velocity can be broken down for the axial velocity v_a and tangential velocity v_θ and radial velocity v_r . v_a produce longitudinal from the effect of heat exchange tube bundle, v_θ produce the effect of horizontal sweep bundles, v_r that secondary flow is generated by the bundle disturbance. the shell side of the three component makes the function of flow between the longitudinal flow and transverse flow, both of the two characteristics: compared with the longitudinal flow, spiral flow of the tangential component of the shell side fluid velocity gradient along the shell radius direction, destroyed the boundary layer on the surface of the heat exchange tube

bundle, enhanced heat transfer; Compared with horizontal flow, spiral flow axial component of the plunger shape is closer to the fluid flow, improve the heat transfer temperature difference.

The shell side of the Figure 8 for the spiral Angle of 40° when convective heat transfer full development period of the velocity vector distribution on cross section. Can see that, because of the continuous helical baffle diversion, formed on the shell side of the fluid in the cross section of regular rotation flow, the distribution of v_θ is evener, compared with the traditional bow baffle plate, eliminates the flow dead zone, and to reduce the impact of the fluid exchange heat pipe bundle.

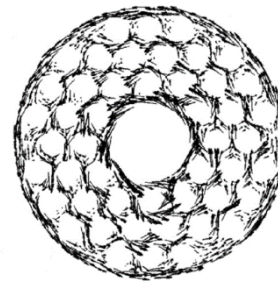


FIGURE 8 The velocity vector distribution on cross section

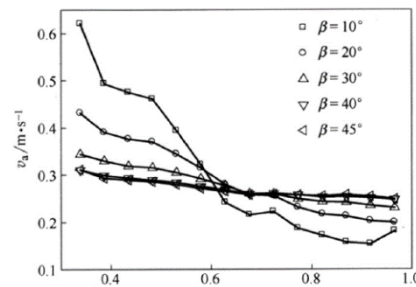


FIGURE 9 Radial distribution of axial velocity along the shell

Bundle between the medial and centre false wall surface and bundle the wall between the lateral and shell because of the heat exchange tube bundle of turbulence effect influence is weak, low flow resistance, fluid showed more significantly than control internal rotation, formed by the spiral flow in two places.

Figure 9 shows the shell side mass flow rate is equal to ($M_s = 4Kg \cdot S^{-1}$), the different spiral Angle v_a . And decreased with the increase of the radial position δ ($\delta = 2r / D_s$), centre near false tube v_a is greater than other location. Spiral Angle at 10, v_a radial along the shell to reduce the sharpest, centre near false tube of shell wall near 4 times, poor distribution uniformity. Gradually, with the increase of helical Angle v_a along the radial distribution even, $\beta \geq 40^\circ$, the radial distribution uniformity along the shell is better. Shell side spiral channels of distribution can be divided into two areas, near the centre of false tube inner regions, the same radial location along with the increase of helical Angle, and the area near the wall of the outer shell, the same radial position is increased along with the increase of helical Angle.

4.4 SURFACE OF HEAT EXCHANGE TUBE HEAT TRANSFER PERFORMANCE OF THE DISTRIBUTION

Equals the Figure 10 for shell side mass flow rate ($M_s = 4Kg \cdot S^{-1}$), different radial position of the surface of the heat exchange tube Q^* , the change rule of dimension 1 in heat $Q^* = Q_\delta / Q_{\delta=0.42}$. Can see, the spiral Angle is not the change rule of similar at the same time, in addition to the false tube closest to the centre of heat exchange tube, the rest of the radial position of the heat exchange tube are less than 1, indicates that the most close to the centre of the fake tubes due to heat exchange tube bundle inside between the centre of false wall surface and side stream, the influence of surface heat exchange tube in the heat more.

With the increase of radial distance, Q^* downward trend, close to the shell by heat exchange tube bundle of the lateral wall and the influence of the side stream of the shell wall, there will be a certain degree of rise. The smaller spiral Angle, change the magnitude of the more severe, the radial heat exchange tube in different radial positions at this time in exchange for heat distribution inhomogeneity between the stronger, the thermal stress is, the greater the this is the problems that should be paid attention to in the design and use of heat exchanger. When $\beta \geq 30^\circ$ the heat transfer between the heat exchange tube in different radial positions distribution uniformity is better.

4.5 ENTROPY GENERATION ANALYSIS

The second law of thermodynamics, points out that all the actual process in the nature are not reversible. Continuous helical baffle heat exchanger as energy transfer device, the heat transfer process is a typical irreversible process, the energy of the irreversible process will inevitably lead to the loss of available energy. The irreversible loss in the heat exchanger is divided into the irreversible loss caused by finite temperature difference heat transfer and fluid flow in the process of overcoming friction resistance caused by irreversible loss, the sum of the total irreversible loss in the heat exchanger.

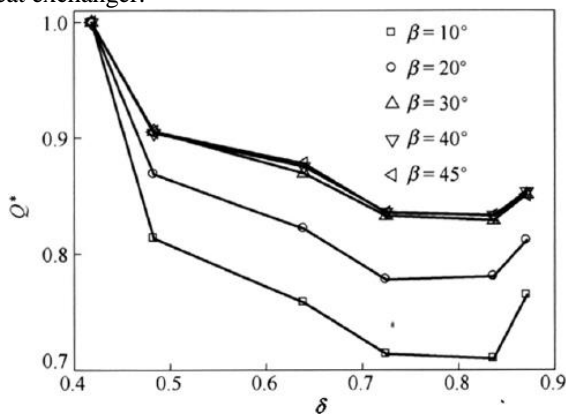


FIGURE 10 Surface of heat exchange tube dimension 1 heat transfer along the radial distribution

The irreversible loss in the heat exchanger can use entropy generation, production rate of heat transfer caused by the entropy is:

$$\dot{S}_{gen,\Delta T} = (Mc_p)_s \ln \frac{T_{s,o}}{T_{s,i}} + (Mc_p)_t \ln \frac{T_{t,o}}{T_{t,i}} \tag{3}$$

For incompressible fluid, Resistance to flow caused by the production rate for entropy is:

$$\dot{S}_{gen,\Delta p} = M_s \frac{\Delta p_s}{\rho_s} \frac{\ln(T_{s,o}/T_{s,i})}{T_{s,o} - T_{s,i}} + M_t \frac{\Delta p_t}{\rho_t} \frac{\ln(T_{s,o}/T_{s,i})}{T_{s,o} - T_{s,i}} \tag{4}$$

Total entropy yield:

$$\dot{S}_{gen} = \dot{S}_{gen,\Delta T} + \dot{S}_{gen,\Delta p} \tag{5}$$

Be-Heat transfer caused by the entropy generation and the ratio of the total entropy generation Can be said in the heat exchanger caused irreversible loss caused by heat transfer and flow resistance of the relative importance of the irreversible loss:

$$Be = \frac{\dot{S}_{gen,\Delta T}}{\dot{S}_{gen}} \tag{6}$$

As shown in Figure 11, when the different helix angle, Be increased with the increase of shell side mass flow is reduced, show that heat transfer caused by irreversible loss percentage of total irreversible loss. In this paper the simulation range, Be less than 0.75, in most cases in 0.9 above, that irreversible loss in the total heat transfer dominates in the irreversible loss. Under small flow rate, the five kinds of helix angle Be were similar, with the increase of flow rate, $\beta = 10^\circ$ when Be falling fastest, $\beta = 20^\circ$ comes second, $\beta \geq 30^\circ$ when Be Dropping lowest. Equals the visible shell side mass flow rate, the smaller helix angle make less of an effect the irreversibility of heat transfer.

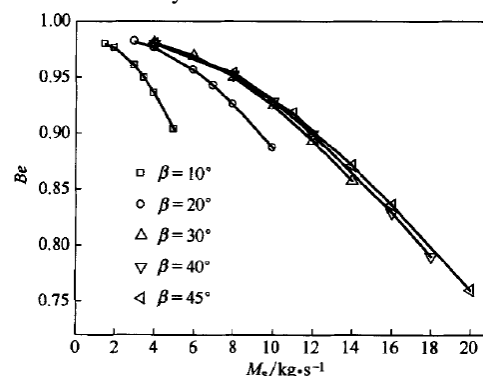


FIGURE 11 Be along with the change of flow rate

For the convenience of comparison of different type of heat exchanger performance under different working conditions, the application needs to be frequently during entropy generation outline 1, entropy generation by the outline 1 is:

$$N_s = \frac{\dot{S}_{gen}}{(Mc_p)_{min}} \tag{7}$$

Entropy generation number is smaller, which indicates that irreversible loss is smaller, the better the performance of heat exchanger.

5 Conclusion

1) The helical Angle is not at the same time, the shell side convective heat transfer in helical channel along the shell axial distribution of different. helical channel after about 1 times the pitch to import export before about 0.75 times as part of the pitch, for the full development period of heat convection.

2) The shell side mass flow rate is equal, the shell side heat transfer coefficient and pressure drop per unit length are along

with the increase of helical Angle decreases, and the decrease of the amplitude is greater than the former, the shell side heat transfer and resistance along with the increase of helical Angle and improve the comprehensive performance.

3) Shell side cross-sectional tangential flow distribution more uniform, but in the centre of the heat exchange tube bundle and false wall between the tube and shell will be formed by the spiral flow in two places.

Acknowledgements

This work was financially supported by the Hunan Science and Technology Foundation Project (2012GK3130).

References

- [1] Bell K 2004 *Journal of Heat Transfer* 6(126) 877-85
- [2] Wang Q W, Chen G D, Chen Q Y 2010 *Heat Transfer Engineering* 10(31) 836-53 (in Chinese)
- [3] Lutcha J, Nemcansky J 1990 *Chemical Engineering Research and Design* A(68) 263-70
- [4] Ji S, Du W J, Cheng L 2009 *Proceedings of the CSEE* 32(29) 60-70 (in Chinese)
- [5] Lei Y G, He Y L, Li R 2008 *Chemical Engineering and Processing* 12(47) 2336-45
- [6] Guo Z-Y, Zhou S-Q, Li Z-X, Chen L-G 2002 Theoretical analysis and experimental confirmation of the uniformity principle of temperature difference field in heat exchanger. *International Journal of Heat and Mass Transfer* 45(10) 2119-27
- [7] Zhao T S 2001 Forced Convection in a Porous Medium Heated by a Permeable Wall Perpendicular to Flow Direction *Journal of Enhanced Heat Transfer* 44 1031-7
- [8] Pesteei S M, Subbarao P M V, Agarwal R S 2005 Experimental study of the effect of winglet location on heat transfer enhancement and pressure drop in fin-tube heat transfer *Applied Thermal Engineering* 25(11-12) 1684-96

Authors	
	<p>Jiazhu Zou, born in June, 1977, Hunan, China</p> <p>Current position, grades: lecturer in Mechanical Engineering, University of South China. University studies: master of engineering in Mechanical Engineering (2006, University of South China, China). Scientific interests: fluid control and computer modeling in mechanical engineering. Publications: 7 papers.</p>
	<p>Fengwei Yuan, born in June, 1977, Hunan, China</p> <p>Current position, grades: associate professor in Mechanical Engineering, University of South China. University studies: master of engineering in Mechanical Engineering (2001, Central South University of Forestry and Technology, China). Scientific interests: virtual reality and computer modeling in mechanical engineering. Publications: 11 papers.</p>
	<p>Qian Deng, born in October, 1987, Hunan, China</p> <p>Current position, grades: lecturer in Mechanical Engineering, University of South China. University studies: master of engineering in Mechanical Engineering (2012, University of South China, China). Scientific interest: computer modeling in Mechanical Engineering. Publications: 4 papers.</p>